Status of coalescing binaries search activities in Virgo

F. Acernese, P. Amico, M. Alshourbagy, F. Antonucci, S. Aoudia, P. Astone, S. Avino, D. Babusci, G. Ballardin, F. Barone, et al.

Status of coalescing binaries search activities in Virgo

F. Acernese[6], P. Amico[10], M. Alshourbagy[11], F. Antonucci [12], S. Aoudia[7], P. Astone[12], S. Avino[6], D. Babusci[4], G. Ballardin[2], F. Barone[6], L. Barsotti[11], M. Barsuglia[8] , Th. S. Bauer[13], F. Beauville[1], S. Bigotta[11], S. Birindelli[11], M.A. Bizouard[8], C. Boccara[9], F. Bondu[7], L. Bosi[10], C. Bradaschia[11], S. Braccini[11], J. F. J. van den Brand[13], A. Brillet[7], V. Brisson[8], D. Buskulic[1], E. Calloni[6], E. Campagna[3], F. Carbognani[2], F. Cavalier[8], R. Cavalieri[2], G. Cella[11], E. Cesarini[3], E. Chassande-Mottin[7], N. Christensen[2], C. Corda[11], A. Corsi[12], F. Cottone[10], A.-C. Clapson[8], F. Cleva[7], J.-P. Coulon[7], E. Cuoco[2], A. Dari[10], V. Dattilo[2], M. Davier[8], M. del Prete[11], R. De Rosa[6], L. Di Fiore[6], A. Di Virgilio[11], B. Dujardin[7], A. Eleuteri[6], M. Evans[2], I. Ferrante[11], F. Fidecaro[11], I. Fiori[2], R. Flaminio[1,2], J.-D. Fournier[7], S. Frasca[12], F. Frasconi[11], L. Gammaitoni[10], F. Garufi[6], E. Genin[2], A. Gennai[11], A. Giazotto[11], G. Giordano[4], L. Giordano[6], R. Gouaty[1], D. Grosjean[1], G. Guidi[3], S. Hamdani[2], S. Hebri[2], H. Heitmann[7], P. Hello[8], D. Huet[2], S. Karkar[1], S. Kreckelbergh[8], P. La Penna[2], M. Laval[7], N. Leroy[8], N. Letendre[1], B. Lopez[2], Lorenzini[3], V. Loriette[9], G. Losurdo[3], J.-M. Mackowski[5], E. Majorana[12], C. N. Man[7], M. Mantovani[11], F. Marchesoni[10], F. Marion[1], J. Marque[2], F. Martelli[3], A. Masserot[1], M. Mazzoni[3], L. Milano[6], F. Menzinger[2], C. Moins[2], J. Moreau[9], N. Morgado[5], B. Mours[1], F. Nocera[2], C. Palomba[12], F. Paoletti[2], 11, S. Pardi[6], A. Pasqualetti[2], R. Passaquieti[11], D. Passuello[11], F. Piergiovanni[3], L. Pinard[5], R. Poggiani[11], M. Punturo[10], P. Puppo[12], S. van der Putten[13], K. Qipiani[6], P. Rapagnani[12], V. Reita[9], A. Remillieux[5], F. Ricci[12], I. Ricciardi[6], P. Ruggi [2], G. Russo[6], S. Solimeno[6], A. Spallicci[7], M. Tarallo[11], M. Tonelli[11], A. Toncelli[11], E. Tournefier[1], F. Travasso[10], C. Tremola[11], G. Vajente [11], D. Verkindt[1], F. Vetrano[3], A. Viceré[3], J.-Y. Vinet[7], H. Vocca[10] and M. Yvert[1]

[1]Laboratoire d'Annecy-le-Vieux de physique des particules (LAPP), IN2P3/CNRS, Université de Savoie, BP 110, F-74941, Annecy-le-Vieux, CEDEX, France;

[2]European Gravitational Observatory (EGO), Via E. Amaldi, I-56021 Cascina (PI) Italia;
[3]INFN - Sezione Firenze/Urbino Via G.Sansone 1, I-50019 Sesto Fiorentino; and/or Università di Firenze, Largo E.Fermi 2, I - 50125 Firenze and/or Università di Urbino, Via S.Chiara, 27 I-61029 Urbino, Italia;
[4]INFN, Laboratori Nazionali di Frascati Via E. Fermi, 40, I-00044 Frascati (Roma) - Italia;
[5]LMA 22, Boulevard Niels Bohr 69622 - Villeurbanne- Lyon Cedex France;
[6]INFN - Sezione di Napoli and/or Università di Napoli "Federico II" Complesso Universitario di Monte S. Angelo Via Cintia, I-80126 Napoli, Italia and/or Università di Salerno Via Ponte Don Melillo, I-84084 Fisciano (Salerno), Italia;
[7]Department Artemis - Observatoire de la Côte d'Azur, BP 42209, 06304 Nice Cedex 4, France;
[8]Laboratoire de l'Accélérateur Linéaire
[8]LAL, Univ Paris-Sud, IN2P3/CNRS, Orsay, France
[9]ESPCI - 10, rue Vauquelin, 75005 Paris - Francee;
[10]INFN Sezione di Perugia and/or Università di Perugia, Via A. Pascoli, I-06123 Perugia - Italiaa;
[11]INFN - Sezione di Pisa and/or Università di Pisa, Via Filippo Buonarroti, 2 I-56127 PISA - Italia;
[12]INFN, Sezione di Roma and/or Università "La Sapienza", P.le A. Moro 2, I-00185, Roma.
[13]National Institute for Nuclear Physics and High Energy Physics, NL-1009 DB Amsterdam and/or Vrije Universiteit, NL-1081 HV Amsterdam, The Netherlands

Abstract. The interferometric gravitational wave detector Virgo is undergoing an advanced phase of its commissioning, during which short runs are routinely performed, where data are analyzed on-line and off-line for the coalescing binaries detection. In this report we present the progresses of the coalescing binaries search activities in Virgo, and we discuss the results of the detection pipelines and veto implementation, using recent data taking

PACS numbers: 04.80.Nn, 95.55.Ym

1. Introduction

The interferometric gravitational wave (GW) detector Virgo is approaching to the end of the commissioning activities and the begin of the long data tacking, scheduled for May 18th 2007[1]. The present detector data are characterized by a high duty cycle and good stability, allowing us to test and setup the detection and veto algorithms and tuning the on-line and off-line computing pipelines. In these conditions it is possible to study the detector stability with respect to specific kinds of searches. In order to not interfere with the ongoing commissioning activity, since September 2006, the collection of science data has been combined during the weekends. Such shot runs are named Weekly Science Run (WSR). In this paper we present the status of the coalescing binaries search activities in Virgo, performed by the coalescing binaries group. In addition we show the relation of the WSR results, obtained with the CB analysis and some aspects of the detector behavior.

2. Weekly Science Run

The periodic weekend data taking usually starts on Friday at 11pm and ends on Monday at 7.00. In figure 1 the calendar of the 6 WSR made in 2006 is reported. Two runs, during October 2006, have been ahead of a time terminated.

The standard goal of these runs is to collect data in 'Science Mode' for 2.5 days, operating without any experiment or activity with the exception of "calibration" and "hardware injection". During such runs we used on-line analysis pipelines, running the h-reconstruction, using Both Multi-Band[2] and Merlino[3] codes. Results obtained are stored for post processing analysis. Part of the results are made available on the web, providing useful information about the detection and the detector status. Acquiring data in controlled conditions permits not only to exercise data analysis procedures but also it gives important feedbacks to commissioning team.

In figure 2 few samples of the overall sensitivity curve of the Virgo detector, acquired during WSR, are shown.

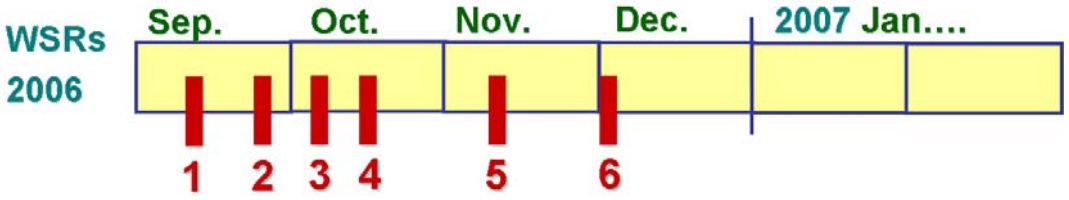

Figure 1. Weekly science run date: WSR1 [September 08-11, 2006] - WSR2 [September 22-25, 2006] - WSR3 [October 06-09, 2006] - WSR4 [October 13-16, 2006] - WSR5 [November 10-13, 2006] - WSR6 [December 01-04, 2006]

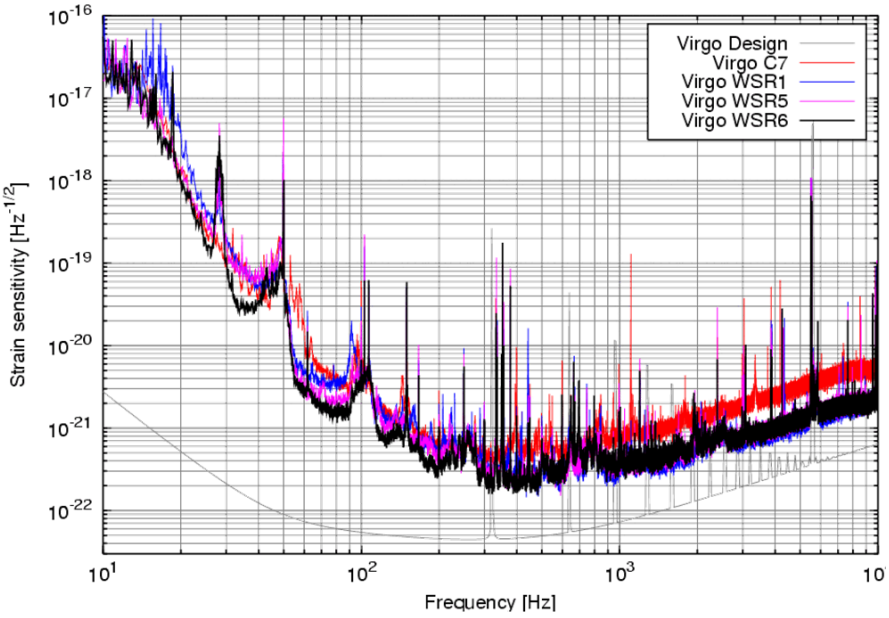

Figure 2. Virgo sensitivity evolution during WSR

3. Duty Cycle and Horizon improvements

It is convenient to describe detector performances in terms of duty cycle and horizon. The lock duty cycle is the percentage time during which the interferometer stays locked. In a similar way we can define science mode duty cycle as the time during which the interferometer stays in science mode.

The science mode duty cycle obtained during these runs was very promising. During the WSR6 (see figure 3) the interferometer operated in science mode the 80.5% of the time. While we had the 2006 record with the WSR1, obtaining a duty cycle of 87.7%.

The Horizon is one of the main index used to quantify the detector performance and amounts to the distance to which an interferometric detector is sensitive to gravitational radiation from a coalescing binary, parameterized on the noise spectrum of the interferometer and the component masses of the binary system. Usually as a reference source a pair of non-spinning 1.4M neutron stars with signal-to-noise ratio equal to 8 is assumed. Finally two different measures of the horizon can be considered with the binary system optimally oriented or not (averaging over time). ‡

In figure 3 we show the horizon evolution during the weekly science runs. It is evident how we had significative horizon improvements between WSR1 and WSR6, roughly estimable about 60%. In particular we obtained in the last run an average horizon of $1.3Mpc$. The long locking periods are also apparent with segments of 15-18 hours. If the detector keeps the actual stability properties and it increases the horizon for the begin of the long science run on May 2007, we will be able to have good quality data to be used in the network of detectors analysis.

‡ There two definitions differ for a constant factor

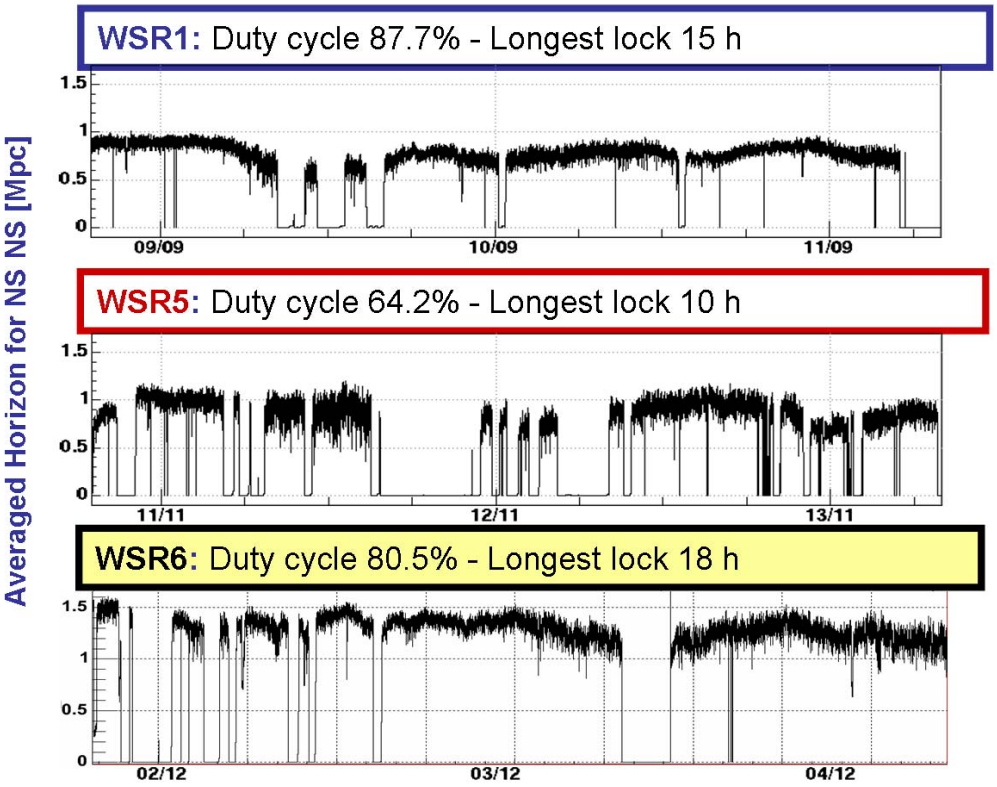

Figure 3. Average horizon distance versus time during the most significative WSR for a $1.4/1.4 Ms$ NSNS binary with SNR = 8. The vertical scale is in Mpc. The science mode duty cycle is also reported on each panel.

3.1. Horizon and the environmental conditions

A dependency of the horizon from the seismic activity due to sea and wind have been recorded during the runs. An empirical relation between these two causes and the horizon was discovered: see figure 4. In the top-right plot we show the sea activity as a function of time, in the bottom-right plot we show the wind activity as a function of time, while in the left plot we show two overlapped curves, representing the horizon. The black curve is the optimal horizon calculated starting as usual form the sensitivity, while the red curve is the horizon estimated combining the two seismic effects.§

In the same figure 4, we observe the horizon falling sometime to zero. Such situations correspond to unlocks of the interferometer, that we can see strongly correlated to seismic activity increase (see arrows).

4. CB Triggers and detector behavior

As previously mentioned, the Virgo coalescing binaries group uses two main pipelines for the on-line analysis. These two pipelines share part of their code: in particular, the

§ At the moment in which this paper is written this effect is no more observable, in particular after the improvements on the Virgo suspensions controls.

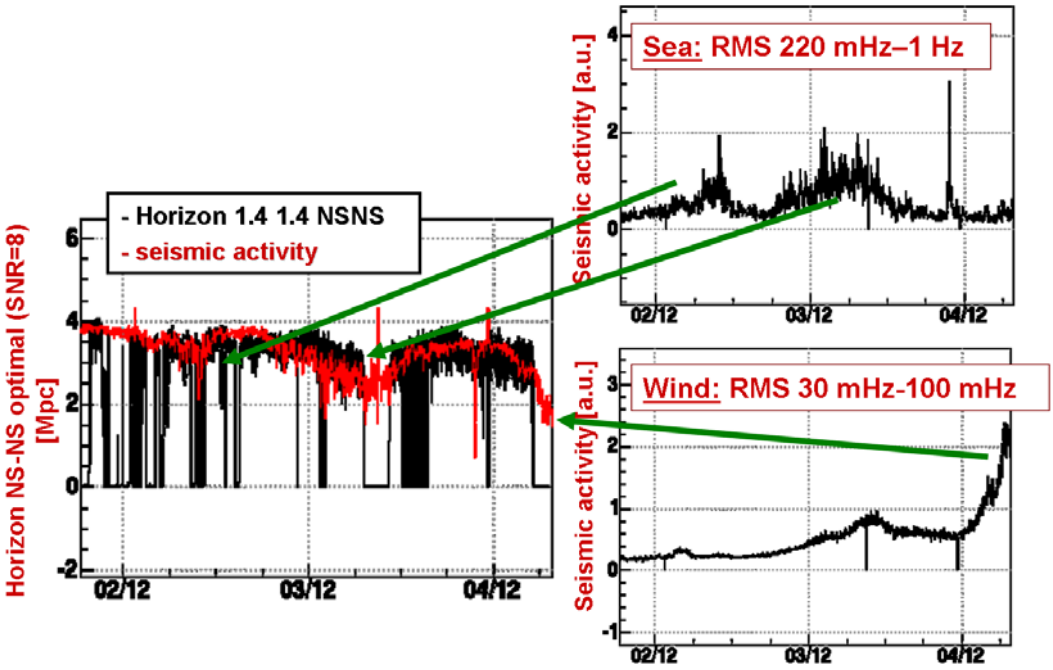

Figure 4. In the upper-right plot the seismic activity due to sea is reported, estimating the RMS in the range $0.221Hz$. In the lower-right plot the seismic activity due to wind is reported, estimating the RMS in the range $0.030.1Hz$. In the left plot the horizon estimated with the detector sensitivity and with the empirical formula is reported.

generation of the templates [4] and of the template grid [5]. Pipelines are configured to use a template bank covering the $[0.9 - 3]Ms$ masses range, with a minimal mismatch of 98%. Triggers are collected with a threshold of 6 in signal-to-noise ratio.

Produced results are stored and used as detector monitor. As a matter of fact, if the signal diverges from gaussianity in frequency region of interest or if it is effected by glitches or other noises, these processes appear in the output stream as triggers. In the upper part of figure 5 the triggers amplitude evolution is shown, obtained during the WSR2. In the lower part of figure 5 the RMS of the output Dark Fringe at 1111Hz for the same epoch is reported. The amplitude of the RMS accounts for the coupling between the frequency noise and the dark fringe signal. Comparing these two plots, a close correlation between the CB signal-to-noise-ratio and the frequency noise is apparent. We note that the amplitude of the recorded trigger was characterized by good stability for the largest part of the run, due to the presence of few peeks with high amplitude. The situation was different in the last part of the data tacking (highlighted with a dashed box in figure 5)where the detector noise increased, leading to an highest signals.

In figure 6 we show the spectra of the above triggers sequence, as further correlation between the CB trigger rate (i.e. the number of triggers produced in unit time) and Virgo detector. This plot provides information about the various contribution coming from different frequencies, providing important information about signal stationarity. As example we can observe the $0.2Hz$ peak, that is correlated to micro seismic activity.

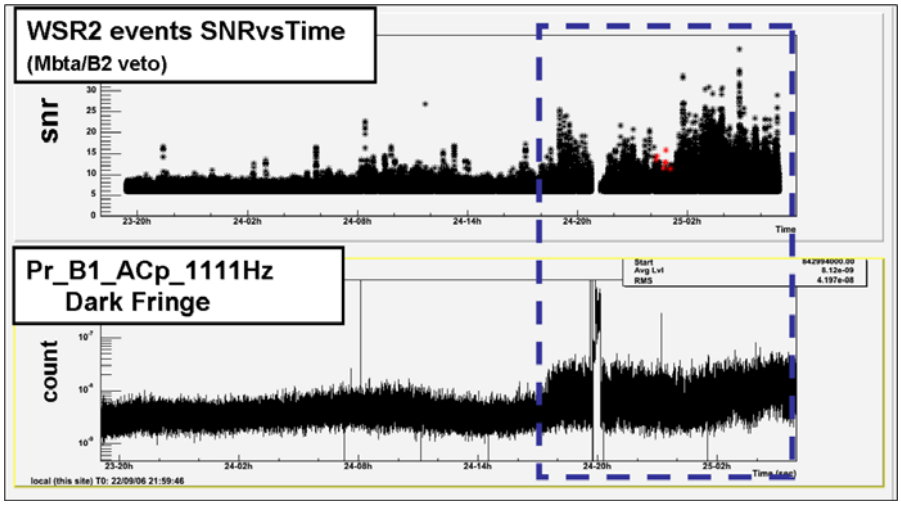

Figure 5. We report in the y-axes the triggers SNR and in the x-axes the time, referred to the WSR2.

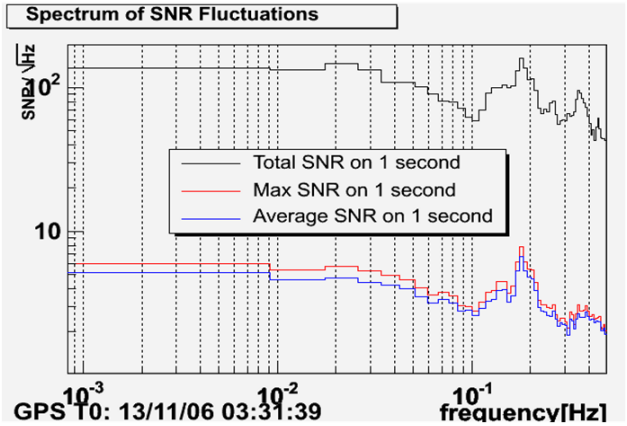

Figure 6. The spectra of the trigger time-series of the WSR2 is reported.

5. Hardware injections

The injection of supernova and coalescing binary signals via hardware into the VIRGO interferometer is one of the main WSR duties. This activity is performed in the first and last night of the run, with the aim of simulating GW effects on the detector and testing the detection pipelines.

Injections are performed acting on the input mirror of the North FabryPerot cavity. A properly shaped force is applied to the test masses, taking into account the electromechanical response of the mirror suspension. The signals generated by BNS, with star masses $m1 = 1.39$ and $m2 = 1.47$, are simulated using a PN2 approximation with a lower frequency cut-off of 50Hz, optimally oriented respect to the detector, and located at a nominal distance of 1.08214 Mpc. The nominal distance has been computed using the sensitivity measured at the time of the injections.

In figure 7 a parameters reconstruction example is shown. For brevity we consider

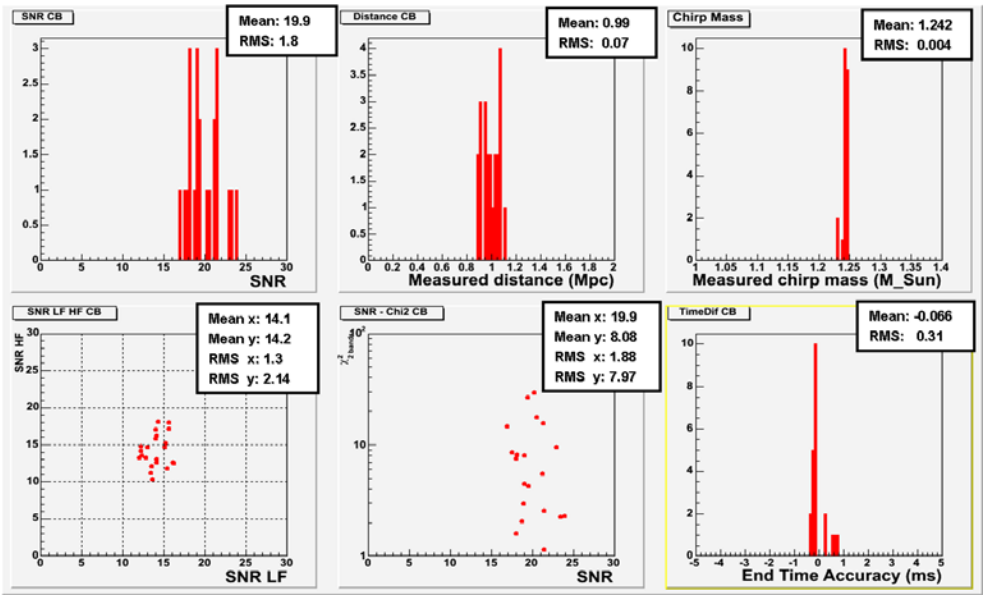

Figure 7. In this plot we show an example of parameter reconstruction, using the hardware injection made in the WSR5 and the mbta analysis code.

only MBTA events, because results with Merlino events are similar.

As can be seen the chirp mass and time accuracy are very well reconstructed. Detailed results on time accuracy have reported in [7] where we show how timing of inspiral signals can be improved using a reference time at a frequency different from the usual time definition.

A discrepancy between the expected reconstructed distance and the obtained one is apparent. The reconstructed value estimated from the detection was $0.99Mpc$, while we expected was $1.08Mpc$. We noticed that bot mbta and merlino pipelines recorded the same result, leading to the cause of such problem. The reason was discovered to be associated to calibration error due to failure in actuation electronics.

Mbta uses two template families, one for the high frequency band and other for the lower frequency band. In the bottom-left of figure 7 the two respective SNR of each bands for all the detected events are shown, confirming the equal distribution of the detected SNR between the two bands.

6. Veto

A relevant percentage of the output triggers is due to the action of the detector noise. Hence, it is important to implement efficient methods in order to reduce this percentage and to select out real triggers produced by coalescing binaries events. A At this aim both pipelines use χ^2 time/frequency veto [6] on-line. The difference between the two approaches is: the Mbta implements a χ^2 with 2 bands, estimated without specific computation, using the information already available from the two bands; the Merlino applies a specific plug-in for the χ^2, configured with 15 bands.

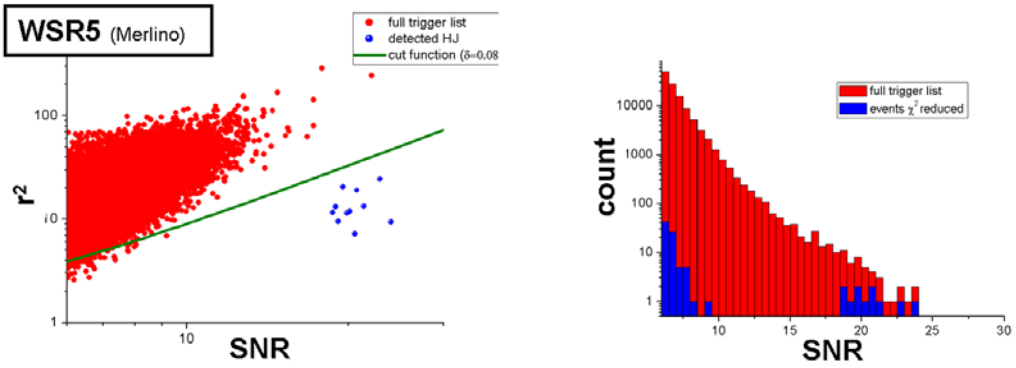

Figure 8. In the left-plot the $SNR\chi^2$ scatter plot is reported, using the WSR6 results. Also the detected hardware injections with SNR around to 20 and the cut function, used to discriminate the events, are shown. In the right plot we present the histogram of the triggers SNR: in red the full trigger list is reported, while in blue the residual list of events below the function $(1 + 0.08\rho^2)$ is reported.

As e.g. in the left plot of figure 8 we show the SNR versus the χ^2 obtained during the WSR5 with the Merlino pipeline. In the plot the group of signals with signal-to-noise ratio around to 20 are associated to CB injections. Due to the high energy of the injections, they appear to be quite well separable from all the other signals associated with noisy events.

In order to use this result as veto, we identify a proper rejection are in such plot, cutting the space $SNR\chi^2$ with a proper function. We can introduce a quadratic function of the SNR $(1 + \delta^2\rho^2)$, where ρ is the SNR of the event and δ is a parameter defined from the required false alarm rate. Applying this veto on the trigger populations, it is possible to reduce drastically the number of false events. In the right plot we show in red the SNR histogram of the original events list and in blue the list of triggers surviving the χ^2 veto procedure. In this case we used a parametric curve with $\delta = 0.08$. In the last distribution the group of injected CB signals is clearly visible, well separated from the triggers associated to noise. In Virgo we perform systematic test on such type of veto, using not only hardware injections but also software injection, covering a wider signals family.

Other veto procedures are possible and have been identified, in particular for what concerns the data quality definition. We implement apriori veto, like monitor for saturation in coil current in NE and WE towers, monitor for picomotors, monitor for SSFS saturation. We are also working on the definition and testing of aposteriori veto. A promising one is the B2 veto, that monitors the power variation in the cavities with the B2 channel signal. In figure 9 we show an example of such veto application, using the WSR2 results. In the left panel the SNR histogram of the full trigger list is reported. In the right panel the SNR histogram of the triggers surviving the B2 veto is reported. In red we identify the CB injected signals. In this case we have a reduction of false alarm of about $\approx 10\%$, removing principally high SNR triggers.

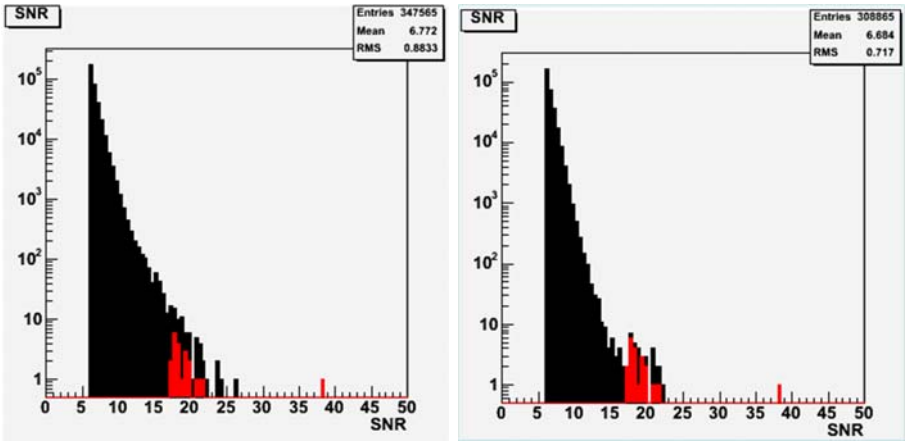

Figure 9. In this panel we show an example of B2 veto application on the WSR2 data. In the left-plot the SNR distribution of the full trigger list is reported. In the right plot the SNR distribution of the triggers, surviving the B2 veto, is reported. In red we highlight the events associated with the detected hardware injections.

7. Conclusions

In 2006 Virgo collaboration decided to start periodically a number of brief science run (called weekly science run) in order to collect useful information for data analysis and commissioning activities. Detector data were characterized by a high duty cycle and a general good stability, allowing us to test and setup the detection and veto algorithms for the on-line and off-line analysis. In this paper we reported a number of results, obtained by the Virgo coalescing binary group. Specifically we presented some results obtained with the mbta and the Merlino detection pipelines. We analyzed the hardware injection, showing the event parameters reconstruction capabilities and some veto technics.

Reference

[1] Acernese F et al, (The Virgo Collaboration), *The status of Virgo*, this proceeding
[2] Marion F et al, (The Virgo Collaboration),*Proceedings of the Rencontres de Moriond 2003*, Gravitational Waves and Experimental Gravity (2004).
[3] Amico P et al, *Computer Physics Communications*, Volume 153, Issue 2, p. 179-189
[4] Bosi L et al, *The Inspiral Library User Manual* A 2004
[5] Beauville F et al, *Class. Quantum Grav.* 20 S789 A 2003
[6] Dow W et al *Phys.Rev. D* , 71 (2005) 062001
[7] Grosjean D et al, (the Virgo collaboration), *This proceeding* "Improving the time accuracy for inspiral signals found by interferometric gravitational wave detectors"